

Retinoic acid signalling in the zebrafish embryo is necessary during pre-segmentation stages to pattern the anterior-posterior axis of the CNS and to induce a pectoral fin bud

Heiner Grandel¹, Klaus Lun¹, Gerd-Jörg Rauch², Muriel Rhinn¹, Tatjana Piotrowski², Corinne Houart³, Paolo Sordino^{3,*}, Axel M. Küchler², Stefan Schulte-Merker², Robert Geisler², Nigel Holder^{3,†}, Stephen W. Wilson³ and Michael Brand^{1,‡}

¹Max Planck Institute for Molecular Cell Biology and Genetics Dresden, Pfotenhauer Strasse 108, 01307 Dresden, Germany

²MPI für Entwicklungsbiologie, Tübingen, Germany

³Department of Anatomy and Developmental Biology, University College London, London, UK

*Present address: Laboratory of Cell Biology, Stazione Zoologica 'Anton Dohrn', Villa Comunale, 80121 Napoli, Italy

†Deceased

‡Author for correspondence (e-mail: brand@mpi-cbg.de)

Accepted 18 March 2002

SUMMARY

A number of studies have suggested that retinoic acid (RA) is an important signal for patterning the hindbrain, the branchial arches and the limb bud. Retinoic acid is thought to act on the posterior hindbrain and the limb buds at somitogenesis stages in chick and mouse embryos. Here we report a much earlier requirement for RA signalling during pre-segmentation stages for proper development of these structures in zebrafish. We present evidence that a RA signal is necessary during pre-segmentation stages for proper expression of the spinal cord markers *hoxb5a* and *hoxb6b*, suggesting an influence of RA on anteroposterior patterning of the neural plate posterior to the hindbrain. We report the identification and expression pattern of the zebrafish *retinaldehyde dehydrogenase2* (*raldh2/aldh1a2*) gene. Raldh2 synthesises retinoic acid (RA) from its immediate precursor retinal. It is expressed in a highly ordered spatial and temporal fashion during gastrulation

in the involuting mesoderm and during later embryogenesis in paraxial mesoderm, branchial arches, eyes and fin buds, suggesting the involvement of RA at different times of development in different functional contexts. Mapping of the *raldh2* gene reveals close linkage to *no-fin* (*nof*), a newly discovered mutant lacking pectoral fins and cartilaginous gill arches. Cloning and functional tests of the wild-type and *nof* alleles of *raldh2* reveal that *nof* is a *raldh2* mutant. By treating *nof* mutants with RA during different time windows and by making use of a retinoic acid receptor antagonist, we show that RA signalling during pre-segmentation stages is necessary for anteroposterior patterning in the CNS and for fin induction to occur.

Key words: *Raldh2*, *no-fin*, Retinoic acid, CNS, Hox genes, Hindbrain, Fin bud, *neckless*, Zebrafish

INTRODUCTION

During vertebrate development retinoic acid (RA) acts in pattern formation and organogenesis. Its synthesis from retinol (vitamin A) requires two sequential oxidative steps. The first step involves the oxidation of retinol to retinal through the action of class IV retinol dehydrogenases (Ang et al., 1996), in a subsequent step, retinal is oxidized to RA. Three retinaldehyde dehydrogenases Raldh1 (Aldh1a1), Raldh2 (Aldh1a2) and Raldh3 (Aldh1a3) operate in vertebrate embryos. *raldh1* and *raldh3* have been detected in primordia of sensory organs in the head (McCaffery et al., 1993; March-Armstrong et al., 1994; Luan et al., 1999; Haselbeck et al., 1999; Grün et al., 2000; Mic et al., 2000; Suzuki et al., 2000), *raldh1* in the pro- and mesonephros (Luan et al., 1999; Haselbeck et al., 1999) and *raldh3* in the limb buds (Grün et

al., 2000). *raldh2* is likewise expressed at distinct sites during organogenesis, but in addition, embryos express *raldh2* during gastrulation and somitogenesis in the paraxial mesoderm in mouse, chicken and *Xenopus* (Niederreither et al., 1997; Swindell et al., 1999; Chen et al., 2001; Niederreither et al., 1997; Niederreither et al., 1999), suggestive of an early role of RA during gastrulation. Upon synthesis, RA is able to bind nuclear ligand-activated transcription factors, the RA receptors alpha, beta, gamma (RAR α , β , γ) that dimerize with RXRs alpha, beta, gamma, thereby modulating transcription in cells of target tissues (Chambon, 1996).

Application of RA to vertebrate embryos or interfering with RA signalling during development affects such diverse organs as the limbs, the branchial arches and the central nervous system. In the developing limb bud, retinoic acid was found to be sufficient (Tickle et al., 1982) and necessary (Helms et al.,

1996; Stratford et al., 1996; Lu et al., 1997) to induce a zone of polarising activity (ZPA). Likewise, the limblessness of *raldh2* mutant mice provides evidence that RA signalling is required for normal limb development (Niederreither et al., 1999).

Different ways of interfering with RA signalling have demonstrated its involvement in the processes that lead to formation of the pharyngeal arches. Generally, caudal arches are strongly affected whereas the anteriormost mandibular arch develops normally. Based on the double knockout of $RAR\alpha$ and $RAR\beta$ as well as upon application of a RA inhibitor, it has been suggested that RA acts on both the endodermal pharyngeal pouches that separate individual arches, and on the mesodermally derived endothelial cells that form the aortic arches (Dupé et al., 1999; Wendling et al., 2000). In addition, neural crest cells that contribute skeletogenic and neurogenic mesenchyme undergo cell death in *raldh2* mutant mice as well as in vitamin A-deficient quail embryos (Maden et al., 1996; Niederreither et al., 2000). Thus RA signalling apparently affects different target tissues that build the arch primordia and is involved in different processes during arch morphogenesis.

The effects of RA signalling on the central nervous system have been analysed in gain-of-function and loss-of-function situations that have generally revealed an involvement of RA signalling in anteroposterior patterning. In gain-of-function studies, the embryos show loss of forebrain and concomitant expansion of the hindbrain and spinal cord (Durstion et al., 1989; Sieve et al., 1990; Simeone et al., 1995; Avantaggiato et al., 1996; Zhang et al., 1996) whereas in loss-of-function experiments it was found that the defects are spatially more restricted to the hindbrain (Maden et al., 1996; Gale et al., 1999; Niederreither et al., 2000; White et al., 2000). It has been proposed that the observed defects are due to modulation of the strength of a posteriorising influence of RA on the nervous system. But while gain-of-function studies have popularised the idea that RA acts as a transforming signal on the newly induced neural tissue, causing posterior transformations and an ordered repatterning along the neuraxis, loss-of-function studies have emphasised that the defects are spatially limited to the posterior hindbrain, which appears anteriorised but does not display midbrain character. In order to explain the defects seen in the hindbrains of mouse and quail embryos that lack RA signalling, it has been proposed that RA acts in a concentration-dependent manner on pattern formation along the anteroposterior extend of the hindbrain. Based on the expression of *raldh2* in the paraxial mesoderm and in the developing somites as well as the presence of *cyp26*, an enzyme that is able to oxidatively inactivate RA in the fore- and midbrain territory (White et al., 1996; Hollemann et al., 1998), a RA diffusion gradient from posterior to anterior was proposed to pattern the presumptive hindbrain (Swindell et al., 1999; Fujii et al., 1997; Hollemann et al., 1998) (for a review, see Gavalas and Krumlauf, 2000).

Experimentally, the presence of a graded posteriorising signal emanating from the somites and the posterior neural tube has been revealed in grafting and transgenic experiments and was characterized to confer positional information which is interpreted by the *hox* genes or other spatially restricted genes such as *Kreisler* in the hindbrain (Itasaki et al., 1996; Grapin-Botton et al., 1997; Grapin-Botton et al., 1998) (see also Gould

et al., 1998). RA is sufficient to mimic this signal as well as necessary to pattern the posterior hindbrain during early somitogenesis in chick (Dupé and Lumsden, 2001). However, the neural tube is already coarsely regionalised at these stages, since the somite-derived posteriorising signal elicits different responses in anterior and posterior hindbrain (Gould et al., 1998; Grapin-Botton et al., 1997; Grapin-Botton et al., 1998). Indeed, Dupé and Lumsden (Dupé and Lumsden, 2001) have shown that anterior hindbrain patterning requires RA during gastrulation. Furthermore grafting experiments have revealed that even though anterior hindbrain can be transformed to a posterior hindbrain fate upon grafting to the appropriate axial level, no part of the hindbrain can be induced to express combinations of posterior spinal cord *hox* genes (Grapin-Botton et al., 1997). It thus appears that patterning of the hindbrain and spinal cord occurs in sequential steps with an increasing degree of pattern refinement as development proceeds.

In the present study we describe the isolation and expression pattern of the *raldh2* gene in zebrafish and the phenotype of the mutant *no-fin* (*nof*) which we find is caused by a mutation in *raldh2*. The *nof* mutant shares the loss of forelimbs (pectoral fins) and posterior branchial arches with the mouse *raldh2* mutant (Niederreither et al., 1999). *nof* mutants differ from *raldh2*^{-/-} mice in the effects on the neural tube, in that the hindbrain is present in *nof* but expanded along the anteroposterior axis. The adjacent spinal cord appears misspecified, at the level of somites one to three as determined by the expression of *hox* marker genes, but also further caudally as revealed by the downregulation of *hoxb6b* in the caudal spinal cord. These findings suggest more widespread effects of RA signalling in the neural tube of the zebrafish than previously thought (Holder and Hill, 1991) and raise the question about the developmental timing of such an overall patterning influence of RA in the embryo. Indeed, by inhibition of RA signalling and early marker analysis we show that RA is required prior to somitogenesis to exert a posteriorising influence on the hindbrain and spinal cord. In addition we find that RA is required during pre-segmentation stages for pectoral fin induction to occur at larval stages. In both cases we could also detect a later function of RA in the affected tissues.

MATERIALS AND METHODS

Fish maintenance

Zebrafish were raised and kept under standard laboratory conditions at about 27°C (Westerfield, 1994; Brand et al., 2002). Mutant carriers were identified by random intercrosses. To obtain mutant embryos, heterozygous mutant carriers were mated. Typically, the eggs were spawned synchronously at dawn of the next morning, and embryos were raised at 28.5°C. In addition, morphological features were used to determine the stage of the embryos, as described by Kimmel et al. (Kimmel et al., 1995).

Isolation and mapping of *raldh2* cDNA, phylogenetic analysis

We sequenced a zebrafish EST-clone with significant sequence similarity to mouse *raldh2* (AI476832, AI477235) and obtained a partial *raldh2* sequence that was truncated at the 5' end. Using the partial C-terminal sequence and degenerate N-terminal primers, we amplified a 5' truncated zebrafish *raldh2* fragment from cDNA. Two

additional ESTs with identical sequences at the 5' end of the coding region and 5' UTR (AW018689, AW184553) allowed extension to the full length sequence (GenBank accession number: AF288764). Subsequently we mapped *raldh2* on the radiation hybrid map as described (Geisler et al., 1999). The phylogenetic tree shown in Fig. 1C is derived from the following sequences: Accession numbers: DmCG3752 AAF52769, HsAldh-E2 AAA51693, MmAldh-E2 P47738, GgAldh1 P27463, HsAldh1 P00352, MmAldh1 AAB32754, XIRaldh2 AF310252, GgRaldh2 AF064253, HsRaldh2 AB015226, MmRaldh2 NM009022, GgAldh6 AAG33934, HsAldh1a3 XP_017971, MmRaldh3 AAF86980, DmCG6309 AAF56646, ScDHAY P32872, DmCG8665 AAF53994, HsAldh9 XP_047474, MmAldh9A NP_064377, CeT05H4.13 T31905, DmCG11140 AAF59247, HsAldh3a1 AAH08892, MmAldh3a1 NP_031462, DrAF254954, DrAF254955, HsAldh3a2 XP_045058, MmAldh3a2 AAH03797, HsAldh3B1 AAH13584, Drest3 – assembled from following ESTs: fi76h10.y1, fj52e12.y1, fi26c02.y1, fi81g03.y1, fb75e12.y1, fc29g10.y1, fr80h10.y1, fi26c02.x1, fi76g10.x1, fr80h10.x1.

Mapping *nof* on the meiotic map

nof was mapped by crossing a Tü mutant carrier with a WIK reference fish (Rauch et al., 1997) and collecting the F₂ offspring. A set of 48 SSLP markers (Knapik et al., 1996) were then tested on pools of 48 mutants and 48 siblings. Linkages from the pools were confirmed and refined by genotyping single embryos. For the marker z8693, we analysed 521 mutant embryos, equivalent to 1042 meioses. For the marker z9273 we analysed 493 mutant embryos, equivalent to 986 meioses.

Whole-mount in situ hybridisation

In situ hybridisations were done as described previously (Reifers et al., 1998). Probes and wild-type expression patterns have already been described: *hoxb5a*, *hoxb6a*, *hoxb6b*, *hoxb4a* (Prince et al., 1998a; Prince et al., 1998b), *val* (Moens et al., 1998), *krx20* (Oxtoby and Jowett, 1993), *pax2.1* (Lun and Brand, 1998).

Injections of synthetic *raldh2* RNA and morpholino oligonucleotide

RNA injections were done as described by Reifers et al. (Reifers et al., 2000). Wild-type and *nof* alleles of *raldh2* mRNA, obtained by in vitro transcription from a pCS2-*raldh2* clone, were injected into 1- to 2-cell stage embryos into the animal pole of the yolk cell just below the cytoplasm. Both clones were truncated at the 5' end by 75 bp. Truncated wild-type mRNA rescued pectoral fin development of *nof* homozygotes thus revealing functionality of the encoded protein. For each injected egg, non-injected controls were kept separately.

To phenocopy the *nof* phenotype, a morpholino oligonucleotide (MO) covering the initiation codon of the *raldh2* gene was injected into the yolk at the 1-cell stage: 5'-GTT CAA CTT CAC TGG AGG TCA TC-3'. Coinjection of wild-type *raldh2* mRNA was used to control for the specificity of this MO.

Alcian Blue stainings, RA treatment and RA inhibitor treatments

Alcian Blue stainings of larval cartilages were done as described by Grandel and Schulte-Merker (Grandel and Schulte-Merker, 1998). To rescue *nof* mutants by application of RA, eggs were incubated from 30% epiboly onwards in E3 medium (Brand et al., 2002) containing 10⁻⁹ M all-*trans* RA (Sigma R2625). This medium was prepared by diluting a 10⁻⁶ M stock solution of all-*trans* RA in DMSO 1:1000 in E3. If RA-containing medium was replaced by E3, the embryos were rinsed several times in E3. Non-treated controls were always kept. BMS493 (Bristol Meyers Squibb) is a pan RAR inhibitor, thereby compromising RA signalling (Wendling et al., 2000; Dupé and Lumsden, 2001). 1×10⁻⁶ and 5×10⁻⁶ M dilutions were prepared in E3.

RESULTS

Isolation of zebrafish *raldh2*

In order to characterise endogenous sites of RA production in the zebrafish, the gene encoding retinaldehyde dehydrogenase 2 (*raldh2*) was cloned by PCR using cDNA from 24-hour embryos. Primers were designed using a partial C-terminal sequence of a zebrafish EST clone matching the *raldh2* sequence of other species and degenerate primers for the N-terminal end. We obtained a partial sequence that could be further extended towards the N-terminal end by alignment with further EST sequences. A comparison of the encoded protein sequence with Raldh2 proteins of other species revealed an overall amino acid sequence identity of 78% (*Xenopus*, chicken, mouse) and 79% (human) (Fig. 1A,B).

A phylogenetic tree constructed from blast search data shows that the cloned gene is more similar to tetrapod *raldh2* genes than to other retinaldehyde/aldehyde dehydrogenases (Fig. 1C). We have mapped the gene to linkage group 7 (Fig. 1D; see below) which is known to be syntenic to the q-arm of human chromosome 15 (Woods et al., 2000; Postlethwait et al., 2000), to which the human orthologues of *raldh2* and *raldh3* have been mapped (<http://www.ncbi.nlm.nih.gov/genome/guide/human/>). The expression pattern of the cloned gene is similar to tetrapod *raldh2* but not to tetrapod *raldh3* (see below).

Thus, synteny, phylogenetic analysis and expression pattern (see below) suggest that we have identified the zebrafish orthologue of tetrapod *raldh2*.

Expression pattern of *raldh2*

We examined the expression pattern of *raldh2* by whole-mount in situ hybridisation. *raldh2* starts to be expressed at 30% epiboly, in a circular domain at the blastoderm margin of the zebrafish embryo (Fig. 2A). At the onset of gastrulation, *raldh2* expression is downregulated in the most dorsal part of the embryo, the embryonic shield (Fig. 2B,C). At 60% epiboly *raldh2* expression becomes downregulated on the ventral side of the embryo and sagittal sections reveal that it is restricted to the involuting paraxial endomesoderm (Fig. 2D,E). During somitogenesis stages, *raldh2* expression is found in the somitic- and lateral plate mesoderm (Fig. 2F,G,H,I). At later stages, *raldh2* is expressed in distinct areas of the embryo such as the eye, the branchial arch primordium, the pronephric duct, in the lateral plate just posterior to the fin buds, and in distinct regions in the brain. At the 20-somite (20s) and later stages restricted expression in the dorso-temporal quadrant of the eye is observed while a very weak domain is located on the ventral side of the eye near the choroid fissure at 26 hours (Fig. 2I,J). At 12s, *raldh2* expression extends from the lateral plate mesoderm into the region where the caudal part of the pharyngeal arch primordium will form (Fig. 2H inset). At 26 hours and later, *raldh2* expression is detected in the post-otic part of the pharyngeal arch primordium, which separates into discrete domains as the gill arches differentiate at 48 hours (Fig. 2K,N). In the trunk myotomes, *raldh2* expression has been downregulated at 26 hours. At this stage, it remains in the ventral part of the tail myotomes (not shown). Cells surrounding the neural tube at the level of somites 3 and 4, express *raldh2* at 26 hours, an expression domain that is also maintained at later stages (Fig. 2Q,R). Expression is also

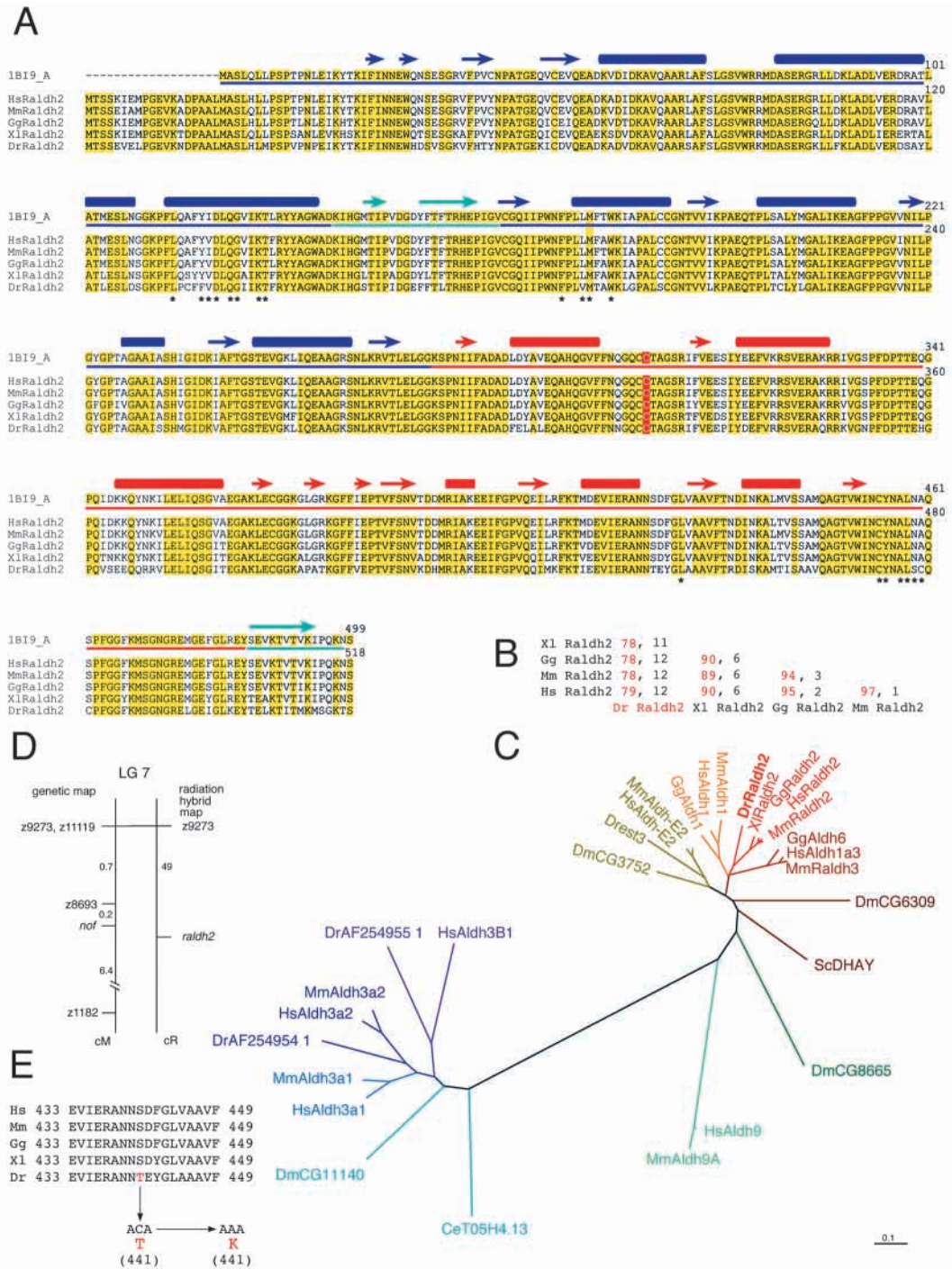


Fig. 1. (A) Sequence alignment of tetrapod and zebrafish *raldh2*. Structural data derived from rat Raldh2/1B19_A. Bars above the sequences denote α helices; arrows, β -sheets. Colour code: blue, nucleotide binding domain; red, catalytic domain; green, tetramerisation domain; the catalytic cysteine is highlighted in red; residues forming the catalytic channel are marked with an asterisk. (B) Table shows percentage sequence identities (red) and sequence similarities (black). (C) Phylogenetic tree constructed from blast search data: Aldh1=Raldh1, Aldh1a3=Aldh6=Raldh3. (D) Genetic and radiation hybrid maps of linkage group 7 showing *nof* and *raldh2* linked to the same marker. (E) The *nof raldh2* allele encodes a Thr to Lys change within the catalytic domain.

detected in a patch of mesenchymal cells beneath the notochord at the axial level of somites 2 and 3 (Fig. 2K). Furthermore, the anterior part of the pronephric duct expresses *raldh2* at 26 hours (Fig. 2K). This domain later expands caudally and *raldh2* expression is detected at 36 hours and at 48 hours along the whole length of the pronephric duct (not shown). *raldh2* expression is also detected in the lateral plate posterior to the pectoral fin buds at 26 hours (Fig. 2K). At this early stage of bud growth, the domain includes the posteriormost mesenchyme of the pectoral fin buds. Later on, no *raldh2* expression is detected in the pectoral fin bud and

lateral plate expression fades (not shown). At 36 hours and 48 hours discrete domains of *raldh2* expression appear in the brain. At 36 hours, *raldh2* starts to be expressed in a subset of cells in the cerebellar anlage (Fig. 2L,M), a domain that also persists to later stages (Fig. 2P). At 48 hours of development, four discrete expression domains of *raldh2*-positive cells appear in the anterior tectum (Fig. 2O,P).

Mapping and sequencing of *nof* and wild-type *raldh2* alleles

We used a high resolution radiation hybrid map (Geisler et al.,

1999) to localise *raldh2* to linkage group 7 at a distance of 49 cR south of the marker z9273. Independently, we mapped the *no-fin* (*nof*) mutant on the meiotic map between the markers z8693 and z1182, also south of z9273, with a map distance of approximately 0.9 cM. Thus *raldh2* and *nof* map in the same region on linkage group 7 (Fig. 1D). The closely apposed map positions and the phenotype of *nof* homozygous embryos (see below) suggested that *nof* might be a mutant in the *raldh2* gene. We therefore sequenced the *raldh2* gene of wild-type and homozygous *nof* mutant embryos and found a C to A transversion in the *nof* allele that causes the exchange of amino acid 441 threonine in the wild-type enzyme to lysine in *nof* embryos (Fig. 1E). The *raldh2* sequences of three wild-type strains (AB, tup lof, Tü) do not show such a polymorphism. Alignment of crystallographic data derived from rat *Raldh2* (Lamb and Newcomer, 1999) with the zebrafish *raldh2* sequence suggests that the threonine to lysine mutation in *nof* affects the protein's catalytic domain (Fig. 1A).

Phenotype of *no-fin* mutants

We isolated the *nof* mutant in a screen for ENU-induced, recessive embryonic visible mutants. Homozygous mutant embryos lack pectoral fin buds on day 2 of development. They also fail to express *dlx2*, an early marker of apical ectodermal ridge (AER) activity in the fin bud (Fig. 3F,H). *dlx2* in situ hybridisation also shows that precursor cells of the posterior cartilaginous gill arches are not detectable (Fig. 3E,G). On day 5 of larval development, living *nof* larvae are generally distinguished from wild-type siblings by the lack of pectoral fins (Fig. 3B,D), lack of tissue in the branchial region (Fig. 3A,C), and an oedema of the heart (Fig. 3A,C). In rare cases we observe pectoral fins of variably reduced size in day 5 *nof* embryos. *nof* embryos also do not form an air-filled swimbladder (Fig. 3A,C) and die during early larval development. Staining mutants and siblings with Alcian Blue shows no cartilage in the pectoral fin region of *nof* homozygotes (Fig. 3J,L). In wild-type embryos the pectoral fin is composed of a proximal shoulder girdle that is attached to the cleithrum, a bone that does not originate from the fin bud, and a distal cartilaginous disc that articulates with the girdle (Fig. 3J) (Grandel and Schulte-Merker, 1998). In *nof* mutant embryos, neither girdle nor disc are formed and the cleithrum, though present, is smaller (Fig. 3L). In *nof* embryos, mandibular and hyoid arches that constitute the jaw are present though sometimes mildly deformed. 32 of 64 homozygous *nof*

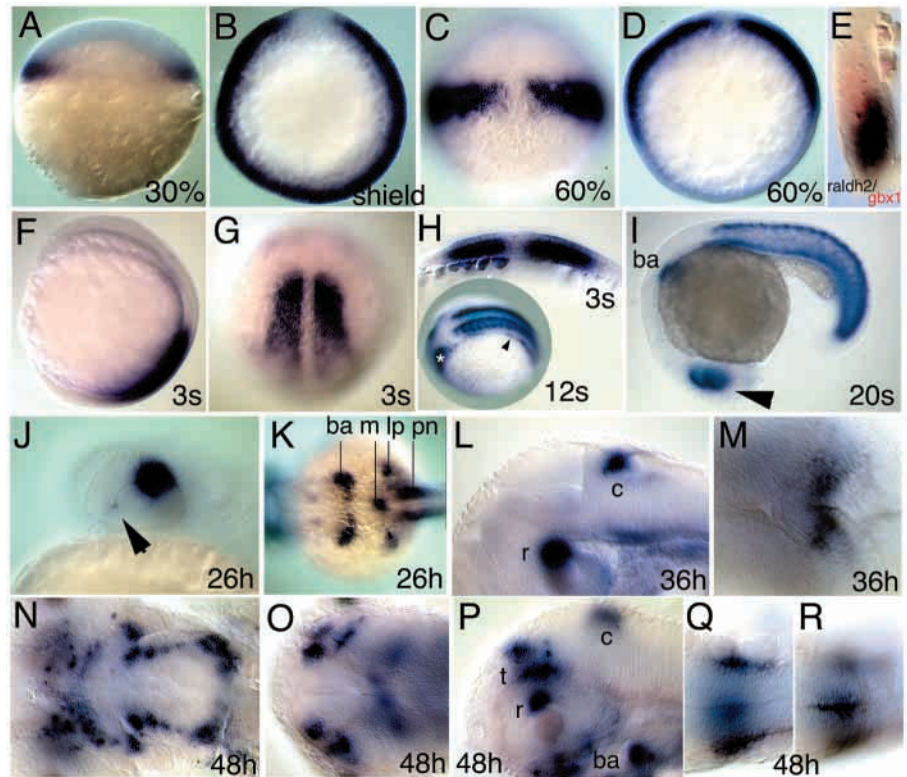


Fig. 2. Whole-mount in situ hybridisations showing *raldh2* expression in the zebrafish embryo and larva at (A) 30% epiboly, (B-E) gastrula, during (F-I) somitogenesis, and (J-R) larval stages. (A) Marginal view, animal pole is upwards. (B,D) Animal view, dorsal is upwards. (C,G) Dorsal view, animal/anterior is upwards. (E) Sagittal section along the animal vegetal axis. (F) Lateral view, anterior is upwards. (H) Cross section perpendicular to anteroposterior axis. (H inset) Dorsolateral view, anterior is to the left. (I,J,L,P) Lateral view, anterior is to the left. (K,M,O,Q,R) Dorsal view, anterior is to the left. (N) Ventral view, anterior is to the left. Note (A) the continuous expression in the blastoderm margin, (B) the exclusion from the shield and (C,D,E) the restriction to the involuting paraxial mesendoderm at 60% epiboly. (E) The sagittal section also reveals positioning of *gbx1* (K. L. and M. B., unpublished) (Rhinn and Brand, 2001) in the neuroectoderm adjacent to *raldh2*. (F,G,H,I) Expression in the somites during somitogenesis stages. (H inset) Expression in the lateral plate mesoderm (arrowhead) extends into the prospective caudal part of the branchial arch primordium (asterisk) at 12s. (I,J) Dorsal expression in the retina (arrowhead) at 20s (I) and 26 hours (J) and weak ventral expression near the choroid fissure at 26 hours (arrowhead). (K) Expression in the caudal part of the branchial arch primordium (ba); in a mesenchymal domain in the midline below the notochord (m), in the anterior part of the pronephric ducts (pn) and in the posterior fin bud- and lateral plate-mesoderm (lp) at 26 hours (arrowhead). (L,M) Expression in the retina (r) and cerebellum (c) at 36 hours. (N-P) Expression at 48 hours. (N) In patches indicating the developing arches; (O) in four domains in the tectum and (P) in the retina (r), cerebellum (c), tectum (t) and branchial arches (ba). (Q,R) Expression surrounding the neural tube at the level of somites 3 to 4.

embryos examined (50%) lacked all five gill arches (branchial arches 3-7, Fig. 3I) while in 16 individuals (25%), remnants of branchial arch 3 and in another 16 embryos (25%), remnants of branchial arches 3 and 4 could be observed (Fig. 3K).

Patterning defects of the spinal cord in *nof* embryos

Defective cranial neural crest-derived branchial arches suggest that RA-dependent anteroposterior patterning of the hindbrain and spinal cord primordia might be more generally affected. *hoxb5a*, *hoxb6a* and *hoxb6b* show an anterior expression limit at the levels of somite one, somite two and somite three, respectively, where strength of expression is most intense

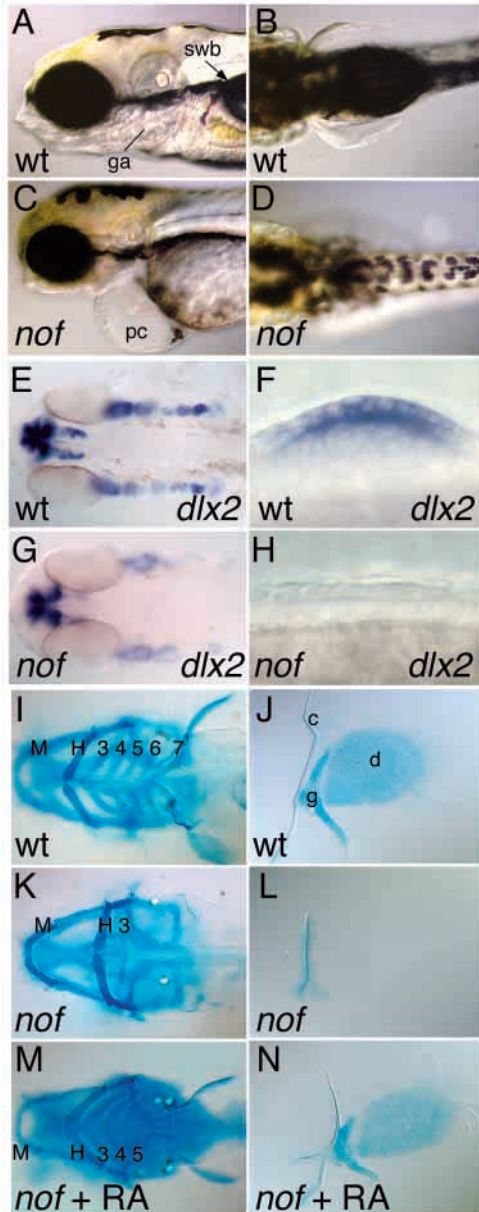


Fig. 3. Phenotype of *nof* homozygotes; wt: wild-type sibling. In A-I,K,M, anterior is to the left; in J,L,N proximal is to the left. (A,C) Lateral, (B,D) dorsal, (E-N) ventral views. (A-D) Larvae on day 5; ga, gill arches; pc, pericardial cavity; swb, swim bladder. (E,G) Branchial arch primordium of 36 hours embryos. (F) Presence and (H) absence of pectoral fin bud and AER marker *dlx2* at 28 hours. (I,K) Cartilage pattern in heads and (J,L) fins of day 5 larvae. M, mandibular and H, hyoid arches; 3-7, gill arches; c, cleithrum; d, distal fin skeleton; g, proximal pectoral girdle. (M) Rescue of arch cartilages and (N) pectoral fins by treatment of *nof* homozygotes with 10^{-9} M retinoic acid at 30% epiboly until 16 hours.

(Prince et al., 1998b). In situ hybridisations on *nof* mutants at the 20s stage reveal downregulation of all three neural tube markers at the anterior end of their expression domains in one quarter of the embryos (Fig. 4A-F). *hoxb6b* expression is reduced along the entire length of its spinal cord expression domain (Fig. 4F). We thus conclude that spinal cord development of *nof* mutants is impaired indicating that *nof*

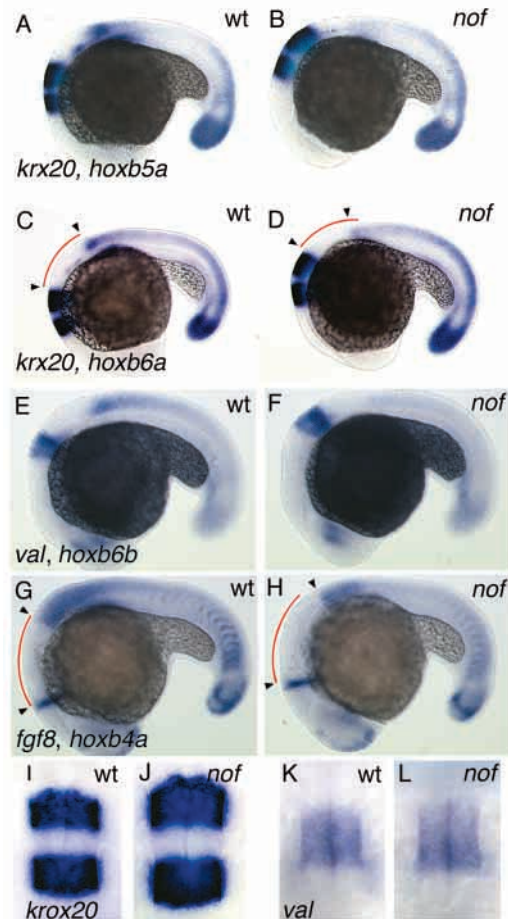


Fig. 4. Anterior-posterior patterning defects in the CNS of *nof* mutants. In situ hybridisation as indicated of wild-type (A,C,E,G,I,K) and *nof* mutant (B,D,F,H,J,L) embryos at the 20s stage. (C,D,G,H) Curved red lines indicate the extent of tissue between different gene expression domains in wild type; arrowheads point to the borders of gene expression in wild type and *nof* mutants.

mutants may be unable to establish the axial characteristics of the wild-type spinal cord.

Patterning defects of the hindbrain of *nof* embryos

In the hindbrain, the expression domains of *hoxb4a*, *valentino* (*val*), and *krox20* (*krx20*) at the 20s stage serve as landmarks of segmentation. The anterior border of the *hoxb4a* domain coincides with the boundary between rhombomeres (r) 6 and r7 (Prince et al., 1998a), *val* marks r5 and r6 (Moens et al., 1998) and *krx20* is expressed in r3 and r5 (Oxtoby and Jowett, 1993). In *nof* mutant eggclays we detect a reduction of *hoxb4a* expression in one quarter of the embryos (Fig. 4G,H). Hindbrain length between areas of *fgf8* or *pax2.1* and *hoxb4a* expression in *nof* mutant embryos is expanded around 12-15% (Fig. 4G,H; Table 1). We also observe a slight expansion of the expression domains of *krx20* and *val* in *nof* embryos compared to wild-type siblings (Fig. 4I-L; Table 1).

We further note a reduction in the distance between the posterior *krx20* stripe and the anterior border of the remaining weak *hoxb6a* expression in the spinal cord of *nof* embryos (Fig. 4C,D). In view of the fact that the anterior spinal cord appears

Table 1. Length differences in *nof* and wild-type hindbrain segments

		r3 <i>krox20</i>	r5 <i>krox20</i>	r5+6 <i>val</i>	r1-6 <i>pax2.1-hoxb4a</i>
Experiment 1	wt	8.7±0.7 (10)	9.5±0.7 (10)	9.6±0.5 (5)	30.4±1.5 (5)
	<i>nof</i>	9.6±0.7 (10)	10.2±0.6 (10)	12.0±0.5 (5)	35.0±1 (5)
Experiment 2	wt	7.6±0.5 (20)	8.1±0.7 (20)	10.8±1.5 (5)	31.6±1.5 (5)
	<i>nof</i>	8.6±0.5 (13)	8.7±0.4 (13)	13.4±0.5 (5)	35.4±2.4 (5)
Increase in segment length in <i>nof</i> in %	Experiment 1	+10%	+7%	+25%	+15%
	Experiment 2	+13%	+7%	+24%	+12%

The length of individual hindbrain segments in wild-type and *nof* embryos was measured in arbitrary units. Numbers in brackets indicate numbers of individuals examined. Values from two independent in situ hybridization experiments per marker are shown and the increase in length of *nof* hindbrain segments are given.

Table 2. Cell numbers in pectoral fin discs in wild-type and retinoic acid treated *nof* embryos

Experiment number	Wild-type siblings			Retinoic acid treated <i>nof</i> embryos		
	No. of embryos	No. of cells AP axis	No. of cells PD axis	No. of embryos	No. of cells AP axis	No. of cells PD axis
1	13	20±1.6	26±2.0	13	20±1.5	26±1.6
2	7	23±0.9	30±1.1	6	24±1.6	30±1.5
3	9	23±2.5	29±1.4	9	23±1.0	30±1.5
4	13	24±1.5	29±1.3	13	24±1.9	31±1.0

Numbers of cells are given along the anteroposterior (AP) and proximodistal (PD) axes of pectoral fin discs in wild-type and retinoic acid-treated *nof* mutants as determined in 4 experiments.

misspecified in *nof* embryos, this finding suggests that the observed hindbrain expansion is directed posteriorly at the expense of spinal cord identities at the level of somites one and two.

Evidence that *nof* is a mutation in *raldh2*

In a first set of experiments, we treated *nof* eggclays with 10⁻⁹ M RA and found that it partially rescues the defects of *nof* mutants. We chose a time window between 30% epiboly and 16 hours for RA treatments, prior to craniofacial neural crest migration (Schilling and Kimmel, 1994) and pectoral fin bud formation (Grandel and Schulte-Merker, 1998) and then washed off RA. We found that RA-treated *nof* mutants develop pectoral fins that contain the proximal girdle and a distal cartilaginous disc (Fig. 3L,N, Fig. 5A,B). The discs of RA-treated *nof* mutants consist of the same number of cells as those of sibling embryos (Table 2), their overall size in RA-treated *nof* embryos is smaller than in RA-treated or untreated sibling embryos (Fig. 3J,N), however, suggesting that the cartilage cells of rescued *nof* embryos are smaller than in wild-type siblings.

Likewise, craniofacial development proceeds further in RA-treated mutants than in untreated controls. In RA-treated embryos, the cartilaginous mandibular and hyoid arches develop normally and branchial arches three and four are regularly observed. In one third of the treated *nof* embryos a fifth arch develops (Fig. 3K,M; Table 3). We did not succeed in rescuing the heart oedema by RA treatment, nor did RA-treated *nof* mutants develop an air filled swimbladder.

In a second set of experiments, we injected 80 pg wild-type *raldh2* mRNA into embryos from *nof* eggclays at the one- to two-cell stage. On day 5, 185/189 larvae (98%) had pectoral fins (Fig. 5C), in one case a pectoral fin formed unilaterally and in three cases, pectoral fins were absent. Inspection of live embryos on day 5 revealed 29 larvae (15%) that apparently lacked tissue in the posterior region of the gill basket and 26 embryos (14%) without an inflated swimbladder. Injecting the equivalent or a 5× higher amount of *nof raldh2* mRNA into one- to two-cell stage embryos from *nof* eggclays failed to rescue pectoral fin development of *nof* embryos. Of 373 embryos injected with 80 pg *nof raldh2* we identified 90 mutants. Of these, 86 (96%) had no pectoral fins on day 5, three

Table 3. Rescue of *nof* pharyngeal arches by retinoic acid treatment

Experiment number	Treated embryos				Untreated control embryos		
	M+H	M+H+3	M+H+3+4	M+H+3+4+5	M+H	M+H+3	M+H+3+4
1	0	0	1	10	4	1	0
2	0	1	17	8	3	3	3
3	0	0	15	2	6	3	0
4	0	0	18	0	10	0	0
5	0	0	7	10	0	2	6
6	0	0	27	0	11	6	6
Σ of embryos	0	1	85	30	11	15	15

Development of cartilaginous pharyngeal arches in *nof* mutant embryos treated with 10⁻⁹ M retinoic acid at 30% epiboly until 16 hours of development, and untreated controls at day 5. The arches that developed are indicated as (M) mandibular arch, (H) hyoid arch, (3, 4, 5) gill arches.

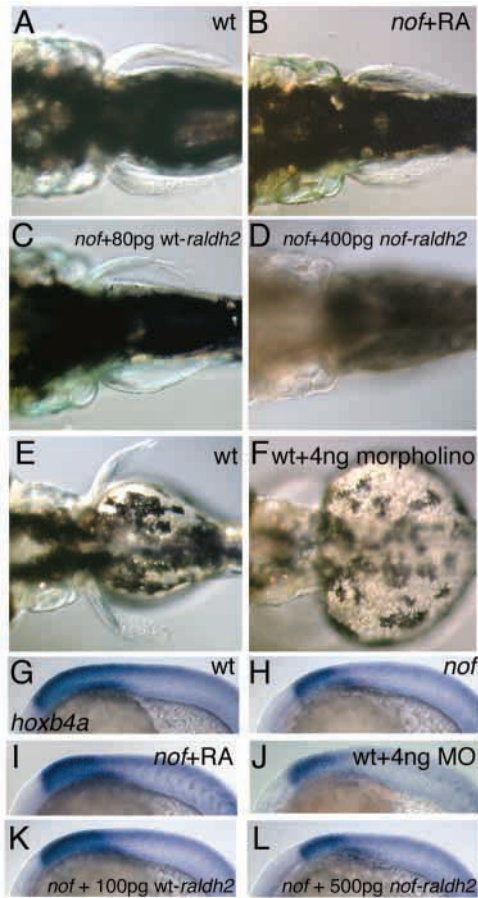


Fig. 5. Dorsal view of pectoral fins on day 5 in (A) a wild-type larva and (B) a *nof* homozygote after treatment with retinoic acid (10^{-9} M, 30% epiboly until 16 hours) and (C) after injection of wild-type *raldh2* mRNA on day 6. (D) Injection of *nof raldh2* mRNA does not provoke fin development in *nof* mutants. (E,F) Pectoral fins on d3 are prominent in wild type (E) but do not develop after injecting a *raldh2*-specific morpholino oligonucleotide (F). *hoxb4a* expression at 20s in wild-type (G) and (H) *nof* sibling embryos. (J,L) Similar *hoxb4a* expression levels as in *nof* homozygotes are detected upon injection of *raldh2*-specific morpholino into wild-type embryos (J) and upon injection of 500 pg mRNA derived from the *nof*-allele of *raldh2* into *nof* homozygotes (L). (I,K) Increase of *hoxb4a* expression levels upon treatment of *nof* homozygotes (I) with retinoic acid (10^{-9} M; 30% until 20s) and (K) injection of 100 pg of wild-type *raldh2* mRNA.

displayed fins unilaterally and one had stumps instead of fins. Of 108 embryos injected with 400 pg of *nof raldh2* we identified 24 mutants, 23 (96%) of which had no pectoral fins. One had stumps instead of fins.

In a third set of experiments we checked expression of *hoxb4a* in the neural tube upon treating *nof* egg-lays with RA or injecting 100 pg wild-type *raldh2*. We identified embryos with *hoxb4a* expression that was intermediate in strength between control wild type and *nof* mutants (compare Fig. 5G,I,K,H). In contrast, injecting 500 pg *nof raldh2* construct into *nof* egg-lays did not improve strength of *hoxb4a* expression in *nof* homozygotes (Fig. 5L).

Using a morpholino oligonucleotide designed to knock down the endogenous *raldh2* message we furthermore show

that the lack of pectoral fins and the reduction of *hoxb4a*, characteristic of *nof* mutants, can be observed after injecting 4 ng of this morpholino oligonucleotide into wild-type embryos (Fig. 5F,J). To control for the specificity of the morpholino-induced phenotype we coinjected 4 ng morpholino and 100 pg of the 5' truncated wild-type *raldh2* mRNA and were able to rescue pectoral fin bud formation (not shown).

Taken together, the rescues of fin development and *hoxb4a* expression in *nof* mutants by RA treatment and wild-type *raldh2* injections, the failure to achieve such rescue with the *nof raldh2* message, and the phenocopy of the *nof* mutant by injecting a morpholino oligonucleotide strongly suggest, that *nof* is a *raldh2* mutant.

Timing of action of RA

Because of the early onset of *raldh2* expression just before gastrulation and its prolonged persistence in the mesoderm during segmentation stages, it is desirable to define more precisely the stages during which RA signalling affects development of the pectoral fins and acts in anteroposterior patterning of the neural tube.

To this end, we have repeated the RA treatments of *nof* egg-lays using four different time windows (Fig. 6; numbers of experimental embryos are listed in the figure). We found that the efficiency with which RA treatments can restore fin development in *nof* embryos dramatically decreases during early somitogenesis stages (Fig. 6C,D). While it is sufficient to treat the embryos prior to segmentation or to start the treatment at the end of gastrulation (tail bud stage) to provoke pectoral fin development, starting treatment at the 10s stage, at best elicits development of stumps instead of fins (Fig. 6D). In these experiments, RA was again washed off long before fin buds appear at 26 hours.

In order to more rigorously test whether a RA signal prior to somitogenesis is sufficient to promote pectoral fin development or whether RA, which might be necessary during early somitogenesis, could have persisted in the embryos after RA had been removed from the medium, we treated wild-type embryos with 1×10^{-6} M BMS493, a pan RAR antagonist (Wendling et al., 2000; Dupé and Lumsden, 2001) (numbers of experimental embryos are listed in Fig. 6), to inhibit RA signalling in wild-type embryos. We were able to block development of a fin bud at 28 hours and the expression of the early AER marker *dlx2*, when starting the inhibitor treatment at 30% epiboly (Fig. 6E,F,G). Most embryos that were left to develop to day 5, failed to form any sign of pectoral fins (Fig. 6I). In contrast, when we started the inhibitor treatment at tail-bud stage most embryos developed fin buds that expressed *dlx2* at 28 hours (Fig. 6H). These buds remained smaller than their wild-type counterparts, however, giving rise only to stumps on day 5 (Fig. 6J). Therefore, a RA signal prior to somitogenesis is essential for initiation of pectoral fin development.

Assaying the expression of molecular markers in the neural tubes of embryos treated with 1×10^{-6} M BMS493 from 30% epiboly onwards reveals a reduction of the *hoxb4a* expression domain at 20s similar to the condition observed in *nof* homozygotes (Fig. 7D). Likewise, hindbrain length increases between the *fgf8* expression domain at the mid-hindbrain border and *hoxb4a* (Fig. 7D). In contrast, embryos receiving 1×10^{-6} M BMS493 treatment from tail-bud stage onwards show only mild reduction of *hoxb4a* expression and no increase

in hindbrain length between the *fgf8* and the *hoxb4a* domains (Fig. 7G). Similarly, the expression domains of *kx20* and *val* at 20s are expanded in experimental embryos treated from 30% epiboly onwards, but not in embryos treated from tail-bud stage onwards (Fig. 7E,F,H,I). Similar results as for *hoxb4a* were obtained with the spinal cord markers *hoxb5a* and *hoxb6b* (Fig. 7E,F,H,I). The behaviour of BMS493-treated embryos suggests that RA acts in a time window situated between 30% epiboly and tail-bud stage in hindbrain and spinal cord patterning.

Early patterning defects of RA deficient embryos

When it became clear that RA signalling acts prior to segmentation to pattern the neuroectoderm, we wished to determine whether we could identify neuroectodermal defects prior to somitogenesis in RA-attenuated/depleted embryos. We have tested the expression of *hoxb1a* and *hoxb1b*, orthologues of the murine *hoxb1* gene, which share an anterior limit of expression at the r3/r4 boundary (McClintock et al., 2001). Based on expression pattern and gain-of-function assays, *hoxb1a* is considered the equivalent of mouse *hoxb1* whereas *hoxb1b* is the proposed equivalent of murine *hoxa1* (McClintock et al., 2001). Importantly, murine *hoxb1* contains a retinoic acid receptor element (RARE) that drives its expression in the presumptive hindbrain and spinal cord of the gastrulating embryo (Marshall et al., 1994; Studer et al., 1998).

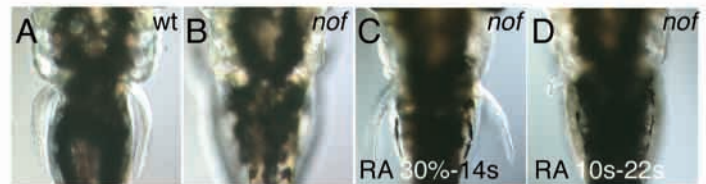
Expression of *hoxb1a* and *hoxb1b* is reduced in *nof* mutants, inhibitor- and morpholino-treated embryos at tail bud stage (Fig. 8A-H). In the case of *hoxb1b* reduced staining was apparent at 80-90% epiboly in inhibitor-treated embryos. *hoxb1a* is not expressed in presumptive rhombomere 5 (McClintock et al., 2001), leaving a gap of unstained cells within the expression domain. In *nof* embryos the position of this gap is still recognisable. It is thus evident that *hoxb1a* expression is strongly affected posterior to rhombomere 5 in RA-depleted embryos (Fig. 8B-D). Double stainings with *otx2* and *hoxb1b* did not show obvious differences in size or strength of the *otx2* domain between *nof* mutants, inhibitor- and morpholino-treated embryos and wild-type embryos. The gap between the two expression domains appears wider in *nof* homozygotes, inhibitor- and morpholino-treated embryos, however (Fig. 8F-H). This suggests that the r3/r4 boundary is pushed posteriorly, possibly as a consequence of the enlarged r3.

Double stainings with *pax2.1* and *val* that indicate the length of the territory between the future isthmus and r5, show a strong increase in hindbrain length at tailbud stage of *nof*, inhibitor- and morpholino-treated embryos (Fig. 8I-L). It should be noted that BMS inhibitor treatment shows a stronger effect than that observed in *nof* or morpholino-treated embryos in this respect. We also note that the distance between r5/r6 as marked by *val* and the anterior tip of the pronephros as marked by *pax2.1* is decreased in all RA attenuated/depleted embryos.

We thus find, in agreement with the late analysis of the CNS in the inhibitor experiments, that neuroectodermal pattern is

retinoic acid treatment at different time-windows

30%	tb	10s	14s	22/23s	larvae show		
					bilateral	unilateral	no fins
[Timeline: 30% to 14s]					23	0	0
[Timeline: 30% to 10s]					43	1	0
[Timeline: 10s to 14s]					19	0	0
[Timeline: 14s to 22/23s]					12	24	39



BMS493 treatments at different time windows

30%	tb	28h/48h	96h	<i>dlx2</i> in apical ectoderm		
				bilateral	unilateral	no exp.
[Timeline: 30% to 28h/48h]				0	2	21
[Timeline: 30% to 14s]				14	5	1
				presence of stumps		
				bilateral	unilateral	no stumps
[Timeline: 30% to 28h/48h]				0	2	20
[Timeline: 30% to 14s]				14	3	5

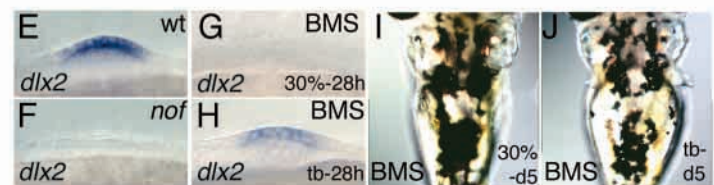


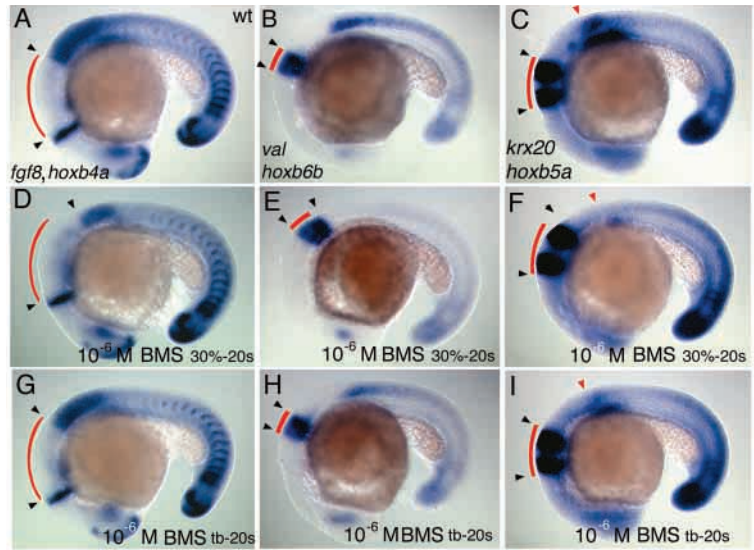
Fig. 6. (A-D) Dorsal view of the pectoral fin region on day 5 in (A) wild-type siblings and (B-D) *nof* mutant embryos. *nof* homozygotes were either (B) not treated or (C,D) treated with 10^{-9} M retinoic acid during the time windows indicated in the table above A-D. (E-H) Ventral view of the pectoral fin buds of (E) wild-type sibling, (F) *nof* and (G,H) BMS493-treated wild-type embryos. (E,H) Fin buds express *dlx2*, indicating AER activity in the apical ectoderm. (F,G) Fin bud regions do not express *dlx2*, indicating lack of AER activity in the ectoderm. (I,J) Dorsal view of the pectoral fin region of BMS493-treated wild-type embryos. Embryos were exposed to 10^{-6} M BMS493 at the different time windows indicated in the table above E-J.

already perturbed at the end of gastrulation in the same way that can still be detected at the end of somitogenesis.

DISCUSSION

We have cloned the zebrafish homologue of the tetrapod *raldh2* gene and report its expression pattern and function during embryogenesis. The early *raldh2* expression phase during pregastrula and gastrula stages in the blastoderm margin and the paraxial mesoderm is consistent with the proposal that RA acts as a posteriorising signal in the neuroectoderm. The later expression phase in distinct organ rudiments suggests a more local involvement of RA during the development of these structures. We have also isolated the *nof* mutant, which contains a point mutation within the catalytic domain of Raldh2. *nof* mutant embryos display

Fig. 7. In situ hybridisations at the 20s stage to visualise the effects of treating wild-type embryos with 10^{-6} M BMS493 during different time windows on the hindbrain and the spinal cord. All panels are lateral views, anterior is to the left. Curved red lines indicate the lengths of hindbrain segments of untreated wild types in all panels. Black arrowheads indicate the true extend of hindbrain segments observed in untreated wild-type (A-C) and experimental embryos. (A,D,G) Expression of *fgf8* and *hoxb4a*; (B,E,H) *val* and *hoxb6b* and (C,F,I) *krx20* and *hoxb5a*. (D,E,F) Inhibition of RA signalling by BMS493 from 30% epiboly onwards expands the hindbrain between the *fgf8* and *hoxb4a* domains, as well as *val* and *krx20* domains; (D,E,F) *hoxb4a*, *hoxb6b* and the anterior part of the *hoxb5a* domain (red arrowhead) are strongly downregulated in the spinal cord. (G,H,I) BMS493 treatments that exclude pre-segmentation stages neither lead to expansion of the hindbrain nor to strong reduction of *hoxb4a*, *hoxb6b* and *hoxb5a*.



phenotypic alterations in the neural tube that are in agreement with the attenuation of a posteriorising signal, most notably an enlargement of the hindbrain at the expense of anterior spinal cord at the level of somites one to three. But also more posterior domains of the spinal cord are affected as detected by a downregulation of *hoxb6b* gene expression along its length. Besides the defects in the neuroectoderm, *nof* embryos show a reduction of the caudal gill arches and a lack of pectoral fins. We have investigated the timing of RA signalling and report its requirement prior to somitogenesis for hindbrain, spinal cord and pectoral fin development.

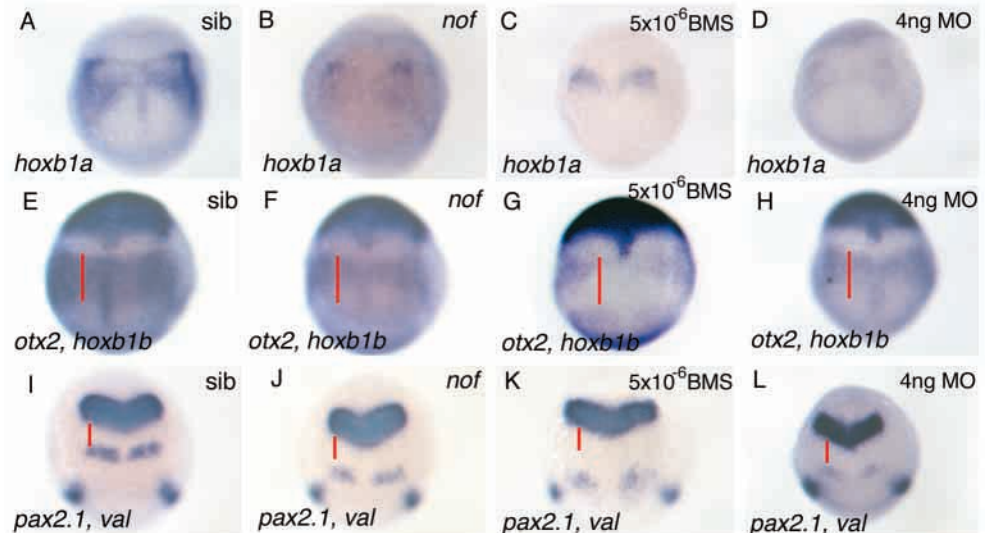
The cloned gene is the zebrafish orthologue of tetrapod *raldh2*

The phylogenetic analysis of blast search data shows that the gene cloned in the present study has the highest sequence homology to tetrapod *raldh2*. It also shows the biphasic expression pattern with an early phase of expression in the paraxial mesoderm during gastrulation characteristic of tetrapod *raldh2* but not *raldh1* or *raldh3*. Moreover, it maps to a location in syntenic chromosomal stretches in fish and human. We therefore conclude that the cloned gene is orthologous to tetrapod *raldh2*.

nof is a mutant in the *raldh2* gene

Several lines of evidence suggest that the *nof* mutant phenotype is caused by a mutation in the *raldh2* gene. First, the positions on the genetic and radiation hybrid maps place *nof* and *raldh2*, respectively, in the same region of linkage group 7. Second, cloning of the *raldh2* allele of *nof* homozygous embryos reveals a point mutation within the catalytic domain of the enzyme which replaces a non polar Thr residue with a positively charged, highly polar Lys residue that is not found in AB, tup lof nor Tü wild-type strains, nor in the published tetrapod sequences. Third, the analysis of the mutant phenotype suggests a defect in RA signalling. *nof* homozygotes lack pectoral fins (forelimbs), posterior branchial arches and show patterning defects in the neural tube as described for tetrapod RA-deficiency models (Niederreither et al., 1999; Maden et al., 1996; Gale et al., 1999). Fourth, application of RA to *nof* mutant embryos is sufficient to rescue branchial arch and pectoral fin development as well as *hoxb4a* expression in the hindbrain. Equally efficient rescues of pectoral fin development and *hoxb4a* expression in the hindbrain are elicited upon injection of *raldh2* mRNA while mRNA of the

Fig. 8. In situ hybridisations at tail bud stage of (A,E,I) wild-type embryos and (B-D,F-H,J-L) embryos with compromised RA signalling. Dorsal views, anterior is to the top. Red lines refer to distances observed in wild-type embryos and are of the same length within each row of embryos. Homozygous *nof*, 5×10^{-6} M BMS493-treated or morpholino-injected embryos downregulate *hoxb1a* (B-D) and *hoxb1b* (F-H) expression compared with wild-type siblings (A,E). (I-L) Length of the prospective hindbrain territory between *pax2.1* and *val* domains is longer in homozygous *nof*, 5×10^{-6} M BMS493-treated or morpholino-injected embryos (J-L) than in wild types (I) at the end of gastrulation.



nof raldh2 allele is ineffective, even when supplied in a 5-fold higher concentration. Taken together the available evidence strongly supports the notion that *raldh2* is mutated in *nof* embryos.

Strength of the *nof* mutation

The observation that wild-type *raldh2* mRNA is able to restore pectoral fin development of *nof* homozygotes while a 5-fold surplus of *nof raldh2* mRNA remains ineffective, suggests that, at least with reference to fin development, the *nof raldh2* allele should be considered non-functional. Expansion of the hindbrain at tailbud stage between the midbrain-hindbrain boundary marker *pax2.1* and the r5/r6 marker *val* appears more pronounced in embryos treated with the pan-RAR inhibitor BMS493 than in *nof* mutants, however, suggestive of an additional source of RA in *nof* embryos. We cannot rule out the presence of an additional *raldh2* allele in zebrafish as linkage group 7 has duplicated during the evolution of fishes (Postlethwait et al., 2000). A different source of RA might be the maternal supply that was found to be in the nanomolar range (Costaridis et al., 1996). We have shown that an external supply of nanomolar concentrations of RA effectively rescues *nof* mutants in vivo. For these reasons, *nof* might not be fully RA deficient.

Similarities and differences in the expression pattern of *raldh2* in zebrafish, mouse, chicken and *Xenopus*

A remarkably conserved feature of *raldh2* expression in tetrapods and zebrafish is its early expression in the paraxial mesoderm during gastrulation and its maintenance in the somites during segmentation stages. In contrast, *raldh1* and *raldh3* are expressed only during organogenesis. The onset of expression differs slightly between species. Zebrafish *raldh2* starts to be expressed shortly before gastrulation in the blastoderm margin while *raldh2* transcripts have not been detected prior to gastrulation in tetrapods (Niederreither et al., 1997; Swindell et al., 1999; Chen et al., 2001).

During late embryonic and larval stages, distinct local foci of *raldh2* expression are seen in tetrapods and zebrafish. Zebrafish larvae display *raldh2* expression in the pronephric ducts as do *Xenopus* and chicken (Chen et al., 2001; Berggren et al., 1999). Another site of zebrafish *raldh2* expression is at early fin bud stages in the lateral plate mesoderm in a domain posterior to the fin bud that includes the posteriormost fin bud mesenchyme as in mouse and chicken (Niederreither et al., 1997; Berggren et al., 1999; Swindell et al., 1999).

In the zebrafish eye, *raldh2* is expressed in the dorsal retina while in tetrapods Raldh1 and Raldh3 were reported to be active in RA production in the dorsal and ventral retina, respectively (reviewed by Dräger et al., 1998). *raldh2* has been detected in the retrolenticular mesenchyme in the mouse (Niederreither et al., 1997), in the retinal pigment epithelium and in a mesenchymal domain dorsal to the eye in the chick (Berggren et al., 1999) whereas Swindell et al. noticed *raldh2* expression in the chick neural retina (Swindell et al., 1999) but did not further investigate the domain of expression. Thus it remains possible that *raldh2* also contributes to RA production in the chick retina. In transgenic zebrafish, a RA-sensitive reporter gene recognises two sources of RA production: the dorsal and ventral retina (Perz-Edwards et al., 2001), thus

revealing a RA distribution in the zebrafish retina analogous to tetrapods. Zebrafish *raldh2* expression is in agreement with the general pattern of RA production in the vertebrate eye (Mey et al., 2001).

The expression of *raldh2* in a subset of cells in the cerebellum starting at 36 hours is surprising because *raldh2* expression was reported to be absent from the fetal cerebellum in the mouse (Yamamoto et al., 1996). Instead, the choroid plexus, which is located immediately caudal to the cerebellum has been shown to contain metabolically active Raldh2 (Yamamoto et al., 1996). We tentatively suggest that the expression domain we identified in the cerebellum of 36 hours and 48 hours old zebrafish larvae demarcates the anlage of the choroid plexus in the zebrafish.

At the 20s stage the caudal part of the branchial arch primordium in zebrafish contains *raldh2* transcripts, which is not the case in mouse and chick, where the branchial arches have been reported to be devoid of *raldh2* transcripts and RA at equivalent stages (Niederreither et al., 1997; Maden et al., 1996). It has been shown in mouse and quail, however, that RA signalling is indispensable for the development of the caudal branchial arches (Niederreither et al., 1999; Maden et al., 1996; Wendling et al., 2000) suggesting that another source of RA serves this function in tetrapods. The fact that we could only rescue the three anterior of the posterior five gill arches by global application of RA to *nof* embryos prior to neural crest migration suggests that, in the zebrafish as in the mouse, *raldh2* is needed in a local context at later times within the arch primordium for the development of the two posteriormost gill arches (Wendling et al., 2000).

We hypothesise that the biphasic expression pattern is indicative of a biphasic activity pattern of *raldh2* that reflects differential functional contexts of RA signalling in the embryo: an early phase shortly before and during gastrulation during which RA produced by *raldh2* may act as a posteriorising factor in global anteroposterior patterning of the embryo, and a second phase of expression, seen during organogenesis stages of development, when transcripts are localised to the primordia of diverse tissues. Here they reflect a local requirement of RA at specifically those sites of expression that may differ among species.

RA signalling is required prior to somitogenesis for pectoral fin induction

The analysis of *nof* homozygotes reveals the requirement of RA signalling for pectoral fin development in fish, as seen with RA-deficient tetrapods (Niederreither et al., 1999). RA has been known to be required for limb development at the time immediately preceding limb bud formation in the chick (Helms et al., 1996; Stratford et al., 1996; Lu et al., 1997). It was therefore surprising to find that RA treatment of *nof* homozygotes effectively rescues fin development only when started before, or at the end of, gastrulation, while such treatments lose their potency during somitogenesis 10 hours before fin buds form. In the reverse experiment, inhibition of RA signalling in wild-type embryos abrogates fin bud and apical ectodermal ridge (AER) formation only, when late blastula and gastrulation stages are included, whereas inhibition from tailbud stage onwards cannot suppress bud and AER formation. These results suggest that a RA signal is necessary prior to somitogenesis for fin induction to occur and

that the tissue receiving this signal loses the competence to do so during the first third of somitogenesis.

Limb induction is the embryologically defined signalling event that causes an AER and, consequently, a limb bud to form. In chick a localised Fgf10 signal originating from the lateral plate mesoderm at prospective bud levels directly elicits AER formation (Ohuchi et al., 1997). Early AER markers are undetectable in *nof* mutants and in *raldh2* mutant mice (Niederreither et al., 1999). The lack of detectable AER activity suggests a loss of the limb induction event in these embryos. This interpretation is further supported by the lack of Fgf10 expression in mouse *raldh2* mutant embryos (Niederreither et al., 1999). A possible explanation of the limblessness observed in *raldh2* mouse and zebrafish mutants is that RA is required for the specification of the mesodermal area that expresses *fgf10* during limb and fin induction.

In addition to the early RA requirement prior to somitogenesis that is essential for fin induction to occur, inhibition of RA signalling after the tail bud stage reveals a post-gastrulation requirement essential for fin bud growth. The fin buds specified after late BMS treatment show retarded growth from early stages onwards such that the resulting appendage is a mere stump. Experiments that locally block RA signalling in the chick at stages immediately prior to limb bud formation likewise demonstrate a late function of RA during limb development (Helms et al., 1996; Stratford et al., 1996; Lu et al., 1997). Nevertheless, development of nearly normal fins is possible in *nof* homozygotes upon early RA treatment. This may reflect the persistence of RA in the embryo after its removal from the medium. Alternatively, another retinaldehyde dehydrogenase may be active in the fin bud. Grün et al. (Grün et al., 2000) have detected *raldh3* in the chick limb bud mesenchyme, which raises the possibility that the overall production of RA in the bud relies on both enzymes. This may explain why the developing fin buds react differently when late *raldh2* activity is reduced (*nof* + early RA) as opposed to blocking total postgastrulation RA signalling (BMS inhibition starting at tail bud stage).

***raldh2* affects hindbrain and spinal cord patterning during pre-segmentation stages**

At the 20s stage, *nof* mutants show a general expansion of the hindbrain between the *pax2.1* or *fgf8* domains at the midbrain-hindbrain boundary and the anterior border of *hoxb4a*, the rhombomere 6/7 boundary. Likewise *krx20*- and *val*-expressing rhombomeres are expanded. The expansion is accompanied by the loss of proper specification of r7 as revealed by downregulation of *hoxb4a*. The anterior part of the expression domains of *hoxb5a* and *hoxb6a* are reduced in strength and *hoxb6b* is downregulated along its whole spinal cord expression domain. As the anterior limit of *hoxb5* expression has been used to mark the rostral edge of the spinal cord (White et al., 2000 and ref. therein), the latter findings indicate that RA signalling also affects anteroposterior patterning in the spinal cord in zebrafish whereas its influence has been proposed to be restricted to the hindbrain alone in tetrapods (Dupé and Lumsden, 2001).

To determine the timing of RA signalling, we used BMS493 to inhibit RAR function. By inhibitor treatments that include late blastula and gastrulation stages we are able to phenocopy the hindbrain and spinal cord defects of *nof* mutants at 20s. In

contrast, inhibitor treatments initiated after gastrulation do not noticeably affect hindbrain markers. Notably, strength of expression of the spinal cord marker *hoxb6b* is nearly normal. Consistent with an effect of RA on the forming neural plate prior to segmentation, in situ hybridisation of RA-depleted embryos shows an expanded hindbrain between the midbrain-hindbrain boundary marker *pax2.1* and the r5/r6 marker *val* at tail bud stage. Furthermore, the *hoxb1a* expression domain loses its 'wings' posterior to r5. It is thus evident that RA signalling affects the neural plate during pre-segmentation stages. In contrast to the chick, where hindbrain domains posterior to the r4/r5 boundary are affected by RA signalling during somitogenesis (Dupé and Lumsden, 2001), RA targets zebrafish neural plate territories posterior to r5 including the spinal cord, prior to somitogenesis. This implicates RA as an early, global regulator of development that influences such different structures and tissues as the neural plate and the fin buds prior to segmentation (Fig. 9). In the context of the neuroectoderm, RA may act in concert with other signals such as Wnt8 (Erter et al., 2001) (K. L., M. R. and M. B., unpublished) to posteriorise the neural plate, a possibility that we currently examine in more detail. The neural tube of zebrafish embryos with compromised RA signalling may thus reveal a state of incomplete posteriorisation.

neckless

An independently isolated ENU-induced zebrafish mutation, *neckless*ⁱ²⁶ (*nls*ⁱ²⁶), likewise is a loss-of-function allele of the *raldh2* gene (Begemann et al., 2001). The name alludes to a reduced distance between the r5 stripe of *krx20* and the *myoD*

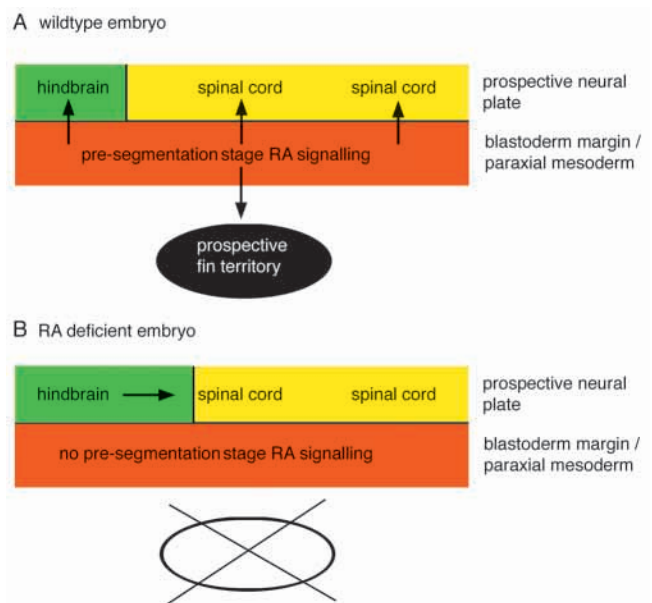


Fig. 9. Schematic diagram of RA action during pre-segmentation stages. (A) RA from the blastoderm margin and/or from the paraxial mesoderm is necessary for correct anteroposterior patterning of the prospective neural plate at hindbrain and spinal cord levels, as well as for fin bud formation. (B) RA signalling is compromised in *no-fin/raldh2*^{-/-} or RAR-inhibited embryos. When RA signalling is blocked during pre-segmentation stages anteroposterior patterning in the neuroectoderm is perturbed, and pectoral fin buds are not induced.

expression domain in the trunk paraxial mesoderm. Similarly, we find a reduced distance between the trunk pronephric mesoderm and the r5/r6 expression domain of *val* (Fig. 8J) in *nof* embryos at tailbud stage prior to somitogenesis. Begemann et al., have attributed this reduction to the lack of short-range RA signalling between the trunk paraxial mesoderm and the tissues of the posterior head. Based on our studies of the *nof* phenotype and even more clearly, of BMS493-inhibited embryos, stained with neuroectodermal markers during gastrulation stages (e.g., Fig. 8I-K), we favour another interpretation, namely that the reduced distance is a consequence of the enlarged hindbrain and can be understood as the consequence of a defective patterning program affecting mostly neural plate posteriorisation by RA prior to somitogenesis.

As observed in *nof*, *nls* embryos lack gill arches, pectoral fin buds and fins and show an expanded *val* domain and a reduced *hoxb4a* staining in the hindbrain. From the phenotypic similarities, a similar map position on LG 7 and the fact that *nls* and *nof* behave similarly in rescue and morpholino experiments, we consider *nof* an allele of *nls*ⁱ²⁶. However, the two mutants complement each other and thus do not behave like alleles (Thomas F. Schilling, personal communication). The tetrameric structure of the enzyme (Lamb and Newcomer, 1999) might explain this behaviour.

Conclusions

The zebrafish *raldh2* gene is expressed during two phases of embryonic development, which reflect distinct functional contexts of RA signalling. During the early phase just prior to and during gastrulation, RA signalling from the blastoderm margin and the involuting paraxial mesoderm is required for proper anteroposterior patterning in the prospective hindbrain and spinal cord and to prime an unknown target tissue, presumably the prospective lateral plate mesoderm, to mediate productive fin induction at later developmental stages. In accordance with the expression pattern, this implies a widespread influence of RA prior to somitogenesis (Fig. 9).

During the second phase *raldh2* is expressed in the anlagen of diverse organs including the somites, the branchial arch primordium and the mesenchyme including and directly posterior to the fin buds. RA mildly influences expression strength of *hoxb4a*, *hoxb5a* and *hoxb6b*, revealing a weak contribution of RA during maintenance of these genes. Furthermore, the posterior two gill arches do not develop after early global application of RA to *nof* embryos. Likewise, pectoral fins do not develop properly from their buds if RA signalling is compromised after gastrulation. This behaviour reveals a later local role for RA in these particular cases.

We thank József Jászai, Florian Raible and Steffen Scholpp for discussions and support, Florence Schlotter for excellent technical assistance, Bianca Habermann for help with the phylogenetic analysis and Fig. 1A, Gerrit Begemann and Phil Ingham for sharing unpublished results and the morpholino oligonucleotide, and Florian Raible and Carl-Philipp Heisenberg for comments on the manuscript. We are grateful to Prof. Pierre Chambon (IGBMC-LGME-U.184-ULPs – Strasbourg) and Bristol Myers Squibb for the gift of BMS 493, and to Vicky Prince for sending *hox* gene probes. This work was supported by the Max Planck Society, by grants from the Deutsche Forschungsgemeinschaft (Bio4-CT98-0309, SCHU1228

and BR17461-3), the European Union (QLRT-2000-02310), EMBO (ALT 415-1996) and the German Human Genome Project (01 KW 9919)

REFERENCES

- Ang, H. L., Deltour, L., Hayamizu, T., Zgombic-Knight, M. and Duester, G. (1996). Retinoic acid synthesis in mouse embryos during gastrulation and craniofacial development linked to class IV alcohol dehydrogenase gene expression. *J. Biol. Chem.* **271**, 9526-9534.
- Avantaggiato, V., Acampora, D., Tuorto, F. and Simeone, A. (1996). Retinoic acid induces stage-specific repatterning of the rostral central nervous system. *Dev. Biol.* **175**, 347-357.
- Begemann, G., Schilling, T. F., Rauch, G.-J., Geisler, R. and Ingham, P. W. (2001). The zebrafish *neckless* mutation reveals a requirement for *raldh2* in mesodermal signals that pattern the hindbrain. *Development* **128**, 3081-3094.
- Berggren, K., McCaffery, P., Dräger, U. and Forehand, C. J. (1999). Differential distribution of retinoic acid synthesis in the chicken embryo as determined by immunolocalization of the retinoic acid synthetic enzyme, RALDH-2. *Dev. Biol.* **210**, 288-304.
- Brand, M., Granato, M. and Nüsslein-Volhard, C. (2002). Keeping and raising zebrafish. In *Zebrafish: A Practical Approach* (eds. C. Nüsslein-Volhard and R. Dahm). Oxford: IRL Press. (in press).
- Chambon, P. (1996). A decade of molecular biology of retinoic acid receptors. *FASEB J.* **10**, 940-954.
- Chen, Y., Pollet, N., Niehrs, C. and Pieler, T. (2001). Increased XRALDH2 activity has a posteriorizing effect on the central nervous system of *Xenopus* embryos. *Mech. Dev.* **101**, 91-103.
- Costaridis, P., Horton, C., Zeitlinger, J., Holder, N. and Maden, M. (1996). Endogenous retinoids in the zebrafish embryo and adult. *Dev. Dynam.* **205**, 41-51.
- Dräger, U. C., Wagner, E. and McCaffery, P. (1998). Aldehyde dehydrogenases in the generation of retinoic acid in the developing vertebrate: a central role of the eye. *J. Nutr.* **128**, 463S-466S.
- Dupé, V., Ghyselinck, N. B., Wendling, O., Chambon, P. and Mark, M. (1999). Key roles of retinoic acid receptors alpha and beta in the patterning of the caudal hindbrain, pharyngeal arches and otocyst in the mouse. *Development* **126**, 5051-5059.
- Dupé, V. and Lumsden, A. (2001). Hindbrain patterning involves graded responses to retinoic acid signalling. *Development* **128**, 2199-2208.
- Durston, A. J., Timmermans, J. P. M., Hage, W. J., Hendriks, H. F. J., de Vries, N. J., Heideveld, M. and Nieuwkoop, P. D. (1989). Retinoic acid causes an anteroposterior transformation in the developing central nervous system. *Nature* **340**, 140-144.
- Erter, C. E., Wilm, T. P., Basler, N., Wright, C. V. E. and Solnica-Krezel, L. (2001). Wnt8 is required in lateral mesodermal precursors for neural posteriorization in vivo. *Development* **128**, 3571-3583.
- Fujii, H., Sato, T., Kaneko, S., Gotoh, O., Fujii-Kuriama, Y., Osawa, K., Kato, S. and Hamada, H. (1997). Metabolic inactivation of retinoic acid by a novel P450 differentially expressed in developing mouse embryos. *EMBO J.* **16**, 4163-4173.
- Gale, E., Zile, M. and Maden, M. (1999). Hindbrain respecification in the retinoid-deficient quail. *Mech. Dev.* **89**, 43-54.
- Gavalas, A. and Krumlauf, R. (2000). Retinoid signalling and hindbrain patterning. *Curr. Opin. Genet. Dev.* **10**, 380-386.
- Geisler, R., Rauch, G.-J., Baier, H., Bebbler, F. v., Broß, L., Dekens, M. P. S., Finger, K., Fricke, C., Gates, M. A., Geiger, H. et al. (1999). A radiation hybrid map of the zebrafish genome. *Nature Genet.* **23**, 86-89.
- Gould, A., Itasaki, N. and Krumlauf, R. (1998). Initiation of rhombomeric *hoxb4* expression requires induction by somites and a retinoid pathway. *Neuron* **21**, 39-51.
- Grandel, H. and Schulte-Merker, S. (1998). The development of the paired fins in the zebrafish (*Danio rerio*). *Mech. Dev.* **79**, 99-120.
- Grapin-Botton, A., Bonnini, M.-A. and Douarin, N. L. (1997). Hox gene induction in the neural tube depends on three parameters: competence, signal supply and paralogue group. *Development* **124**, 849-859.
- Grapin-Botton, A., Bonnini, M.-A., McNaughton, L. A., Krumlauf, R. and Douarin, N. L. (1995). Plasticity of transposed rhombomeres: Hox gene induction is correlated with phenotypic modifications. *Development* **121**, 2707-2721.

- Grapin-Botton, A., Bonnin, M.-A., Sieweke, M. and Douarin, N. L.** (1998). Defined concentrations of a posteriorizing signal are critical for *MafB/Kreisler* segmental expression in the hindbrain. *Development* **125**, 1173-1181.
- Grün, F., Hirose, Y., Kawachi, S., Ogura, T. and Umesono, K.** (2000). Aldehyde dehydrogenase 6, a cytosolic retinaldehyde dehydrogenase prominently expressed in sensory neuroepithelia during development. *J. Biol. Chem.* **275**, 41210-41218.
- Haselbeck, R. J., Hoffmann, I. and Duester, G.** (1999). Distinct functions for *aldh1* and *Raldh2* in the control of ligand production for embryonic retinoid signalling pathways. *Dev. Genet.* **25**, 353-364.
- Helms, J. A., Kim, C. H., Eichele, G. and Thaller, C.** (1996). Retinoic acid signalling is required during early chick limb development. *Development* **122**, 1385-1394.
- Holder, N. and Hill, J.** (1991). Retinoic acid modifies development of the midbrain-hindbrain border and affects cranial ganglion formation in zebrafish embryos. *Development* **113**, 1159-1170.
- Holleman, T., Chen, Y., Grunz, H. and Pieler, T.** (1998). Regionalized metabolic activity establishes boundaries of retinoic acid signalling. *EMBO J.* **17**, 7361-7372.
- Itasaki, N., Sharpe, J., Morrison, A. and Krumlauf, R.** (1996). Reprogramming *hox* expression in the vertebrate hindbrain: influence of paraxial mesoderm and rhombomere transposition. *Neuron* **16**, 487-500.
- Kimmel, C. B., Ballard, W. W., Kimmel, S. R., Ullmann, B. and Schilling, T. F.** (1995). Stages of Embryonic development of the zebrafish. *Dev. Dynam.* **203**, 253-310.
- Knapik, E. W., Goodman, A., Atkinson, O. S., Roberts, C. T., Shiozawa, M., Sim, C. U., Weksler-Zangen, S., Trolliet, M. R., Futrell, C., Innes, B. A. et al.** (1996). A reference cross DNA panel for zebrafish (*Danio rerio*) anchored with simple sequence length polymorphisms. *Development* **123**, 451-460.
- Lamb, A. L. and Newcomer, M. E.** (1999). The structure of retinal dehydrogenase type II at 2.7 Å resolution: Implications for retinal specificity. *Biochemistry* **38**, 6003-6011.
- Lu, H.-C., Revelli, J.-P., Goering, L., Thaller, C. and Eichele, G.** (1997). Retinoid signalling is required for the establishment of a ZPA and for the expression of *hoxb8*, a mediator of ZPA formation. *Development* **124**, 1643-1651.
- Luan, H. and Duester, G.** (1999). Retinoic acid biosynthetic enzyme *Aldh1* localizes in a subset of retinoid-dependent tissues during *Xenopus* development. *Dev. Dynam.* **215**, 264-272.
- Lun, K. and Brand, M.** (1998). A series of no isthmus (*noi*) alleles of the zebrafish *pax2.1* gene reveals multiple signalling events in development of the midbrain-hindbrain boundary. *Development* **125**, 3049-3062.
- McClintock, J. M., Carlson, R., Mann, D. M. and Prince, V. E.** (2001). Consequences of *hox* gene duplication in the vertebrates: an investigation of the zebrafish *hox* paralogue group 1 genes. *Development* **128**, 2471-2484.
- Maden, M., Gale, E., Kostetskii, I. and Zile, M.** (1996). Vitamin A-deficient quail embryos have half a hindbrain and other neural defects. *Curr. Biol.* **6**, 426-447.
- Marshall, H., Studer, M., Pöpperl, H., Aparicio, S., Kuroiwa, A., Brenner, S. and Krumlauf, R.** (1994). A conserved retinoic acid response element required for early expression of the homeobox gene *hoxb1*. *Nature* **370**, 567-571.
- Marsh-Armstrong, N., McCaffery, P., Gilbert, W., Dowling, J. E. and Dräger, U. C.** (1994). Retinoic acid is necessary for development of the ventral retina in zebrafish. *Proc. Natl. Acad. Sci. USA* **91**, 7286-7290.
- McCaffery, P., Posch, K. C., Napoli, J. L., Gudas, L. and Dräger, U. C.** (1993). Changing patterns of the retinoic acid system in the developing retina. *Dev. Biol.* **158**, 390-399.
- Mey, J., McCaffery, P. and Klemeit, M.** (2001). Sources and sink of retinoic acid in the embryonic chick retina: distribution of aldehyde dehydrogenase activities, CRABP-I, and sites of retinoic acid inactivation. *Dev. Brain Res.* **127**, 135-148.
- Mic, F., Molotov, A., Fan, X., Cuenca, A. E. and Duester, G.** (2000). *Raldh3*, a retinaldehyde dehydrogenase that generates retinoic acid, is expressed in the ventral retina, otic vesicle and olfactory pit during mouse development. *Mech. Dev.* **97**, 227-230.
- Moens, C. B., Cordes, S. P., Giorgianni, M. W., Barsh, G. S. and Kimmel, C. B.** (1998). Equivalence in the genetic control of hindbrain segmentation in fish and mouse. *Development* **125**, 381-391.
- Niederreither, K., McCaffery, P., Dräger, U. C., Chambon, P. and Dollé, P.** (1997). Restricted expression and retinoic acid-induced downregulation of the retinaldehyde dehydrogenase type 2 (*Raldh-2*) gene during mouse development. *Mech. Dev.* **62**, 67-78.
- Niederreither, K., Subbarayan, V., Dollé, P. and Chambon, P.** (1999). Embryonic retinoic acid synthesis is essential for early mouse post-implantation development. *Nature Genet.* **21**, 444-448.
- Niederreither, K., Vermot, J., Schuhbauer, B., Chambon, P. and Dollé, P.** (2000). Retinoic acid synthesis and hindbrain patterning in the mouse embryo. *Development* **127**, 75-85.
- Ohuchi, H., Nakagawa, T., Yamamoto, A., Araga, A., Ohata, T., Ishimaru, Y., Yoshioka, H., Kuwana, T., Nohno, T., Yamasaki, M. et al.** (1997). The mesenchymal factor, FGF10, initiates and maintains the outgrowth of the chick limb bud through interaction with FGF8, an apical ectodermal factor. *Development* **124**, 2235-2244.
- Oxtoby, E. and Jowett, T.** (1993). Cloning of the zebrafish *krox-20* gene (*krx-20*) and its expression during hindbrain development. *Nucleic Acids Res.* **21**, 1087-1095.
- Perz-Edwards, A., Hardison, N. L. and Linney, E.** (2001). Retinoic acid-mediated gene expression in transgenic reporter zebrafish. *Dev. Biol.* **229**, 89-101.
- Postlethwait, J. H., Woods, I. G., Ngo-Hazelett, P., Yan, Y.-L., Kelly, P. D., Chu, F., Huang, H., Hill-Force, A. and Talbot, W.** (2000). Zebrafish comparative genomics and the origin of vertebrate chromosomes. *Genome Res.* **10**, 1890-1902.
- Prince, V. E., Moens, C. B., Kimmel, C. B. and Ho, R. K.** (1998a). Zebrafish *hox* genes: expression in the hindbrain region of wild-type and mutants of the segmentation gene, *valentino*. *Development* **125**, 393-406.
- Prince, V., Joly, L., Ekker, M. and Ho, R. K.** (1998b). Zebrafish *hox* genes: genomic organization and modified colinear expression patterns in the trunk. *Development* **125**, 407-420.
- Rauch, G. J., Granato, M. and Haffter, P.** (1997). A polymorphic zebrafish line for genetic mapping using SSLPs on high-percentage agarose gels. *Technical Tips Online* **TO1208** (1997).
- Reifers, F., Böhlh, H., Walsh, E. C., Crossley, P. H., Stainier, D. Y. R. and Brand, M.** (1998). *Fgf8* is mutated in zebrafish *acerebellar* (*ace*) mutants and is required for maintenance of midbrain-hindbrain boundary development and somitogenesis. *Development* **125**, 2381-2395.
- Reifers, F., Adams, J., Mason, I. J., Schulte-Merker, S. and Brand, M.** (2000). Overlapping and distinct functions provided by *fgf17*, a new zebrafish member of the *Fgf8/17/18* subgroup of *Fgfs*. *Mech. Dev.* **99**, 39-49.
- Rhinn, M. and Brand, M.** (2001). The midbrain-hindbrain boundary organizer. *Curr. Opin. Neurobiol.* **11**, 34-42.
- Schilling, T. F. and Kimmel, C. B.** (1994). Segment and cell type lineage restrictions during pharyngeal arch development in the zebrafish embryo. *Development* **120**, 483-494.
- Simeone, A., Avantaggiato, V., Moroni, M. C., Mavilio, F., Arra, C., Cotelli, F., Nigro, V. and Acampora, D.** (1995). Retinoic acid induces stage-specific antero-posterior transformation of rostral central nervous system. *Mech. Dev.* **51**, 83-98.
- Sive, H. L., Draper, B. W., Harland, R. M. and Weintraub, H.** (1990). Identification of a retinoic acid-sensitive period during primary axis formation in *Xenopus laevis*. *Genes Dev.* **4**, 932-942.
- Stratford, T., Horton, C. and Maden, M.** (1996). Retinoic acid is required for the initiation of outgrowth in the chick limb bud. *Curr. Biol.* **6**, 1124-1133.
- Studer, M., Gavalas, A., Ariaz-McNaughton, L., Rijli, F. M., Chambon, P. and Krumlauf, R.** (1998). Genetic interactions between *hoxa1* and *hoxb1* reveal new roles in regulation of early hindbrain patterning. *Development* **125**, 1025-1036.
- Suzuki, R., Shinntani, T., Sakuta, H., Kato, A., Ohkawara, T., Osumi, N. and Noda, M.** (2000). Identification of *Raldh-3*, a novel retinaldehyde dehydrogenase, expressed in the ventral region of the retina. *Mech. Dev.* **98**, 37-50.
- Swindell, E. C., Thaller, C., Sochanathan, S., Petkovich, M., Jessel, T. M. and Eichele, G.** (1999). Complementary domains of retinoic acid production and degradation in the early chick embryo. *Dev. Biol.* **216**, 282-296.
- Tickle, C., Alberts, B., Wolpert, L. and Lee, J.** (1982). Local application of retinoic acid to the limb bud mimics the action of the polarizing region. *Nature* **296**, 564-566.
- Wendling, O., Dennefeld, C., Chambon, P. and Mark, M.** (2000). Retinoid signalling is essential for patterning the endoderm of the third and fourth pharyngeal arches. *Development* **127**, 1553-1562.

- Westerfield, M.** (1994). *The Zebrafish Book*. Edition 2.1. Oregon: University of Oregon Press.
- White, J. A., Guo, Y.-D., Baetz, K., Bekett-Jones, B., Bonasorot, J., Hsu, K. E., Dilworth, F. J., Jones, G. and Petkovich, M.** (1996). Identification of the retinoic acid-inducible all-*trans*-retinoic acid 4-hydroxylase. *J. Biol. Chem.* **47**, 29922-29927.
- White, J. C., Highland, M., Kaiser, M. and Clagett-Dame, M.** (2000). Vitamin A deficiency results in the dose-dependent acquisition of anterior character and shortening of the caudal hindbrain of the rat embryo. *Dev. Biol.* **220**, 263-284.
- Woods, I., Kelly, P. D., Chu, F., Ngo-Hazelett, P., Yan, Y.-L., Huang, H., Postlethwait, J. and Talbot, W. S.** (2000) A comparative map of the zebrafish genome. *Genome Res.* **10**, 1903-1914.
- Yamamoto, M., McCaffery, P. and Dräger, U.** (1996). Influence of the chorioid plexus on cerebellar development: analysis of retinoic acid synthesis. *Dev. Brain Res.* **93**, 182-190.
- Zhang, Z., Balmer, J. E., Lovlie, A., Fromm, S. H. and Blomhoff, R.** (1996). Specific teratogenic effects of different retinoic acid isomers and analogs in the developing anterior central nervous system of zebrafish. *Dev. Dynam.* **206**, 73-86.